
Soft-QMIX: Integrating Maximum Entropy For Monotonic Value Function Factorization

Wentse Chen
Carnegie Mellon University
wentsec@andrew.cmu.edu

Shiyu Huang
Zhipu AI
shiyu.huang@aminer.cn

Jeff Schneider
Carnegie Mellon University
jeff4@andrew.cmu.edu

Abstract

Multi-agent reinforcement learning (MARL) tasks often utilize a centralized training with decentralized execution (CTDE) framework. QMIX is a successful CTDE method that learns a credit assignment function to derive local value functions from a global value function, defining a deterministic local policy. However, QMIX is hindered by its poor exploration strategy. While maximum entropy reinforcement learning (RL) promotes better exploration through stochastic policies, QMIX’s process of credit assignment conflicts with the maximum entropy objective and the decentralized execution requirement, making it unsuitable for maximum entropy RL. In this paper, we propose an enhancement to QMIX by incorporating an additional local Q-value learning method within the maximum entropy RL framework. Our approach constrains the local Q-value estimates to maintain the correct ordering of all actions. Due to the monotonicity of the QMIX value function, these updates ensure that locally optimal actions align with globally optimal actions. We theoretically prove the monotonic improvement and convergence of our method to an optimal solution. Experimentally, we validate our algorithm in matrix games, Multi-Agent Particle Environment and demonstrate state-of-the-art performance in SMAC-v2.¹

1 Introduction

In the context of solving cooperative tasks using deep multi-agent reinforcement learning (MARL), a standard approach is centralized training with decentralized execution (CTDE) [5, 23, 15]. Decentralized execution implies that during the execution phase, the decision-making of each agent is independent and limited to conditioning on local observations. Centralized training, on the other hand, allows the algorithm to access joint actions and global states while training the value function. Compared to decentralized training, which treats other agents as part of the environment, centralized training helps alleviate the instability often encountered in MARL training [30].

In most cooperative tasks, the multi-agent system receives a single joint reward, and MARL algorithms learn the corresponding joint value function based on this reward. Consequently, there is a need to design a credit assignment mechanism [2] that decomposes the joint value function into several local value functions, guiding the updates of the actor networks through these local value functions. The challenge in credit assignment lies in reconstructing the joint distribution from the combination of multiple marginal distributions, a process that typically involves approximation errors [32]. Therefore, past research has primarily focused on exploring the impact of mechanism design on the model’s capacity [27, 31].

Beyond model capabilities, exploration ability is also a critical factor affecting the performance of MARL algorithms. Maximum entropy RL [14], known for encouraging exploration [7], smoothing

¹Our code: <https://github.com/WentseChen/Soft-QMIX>

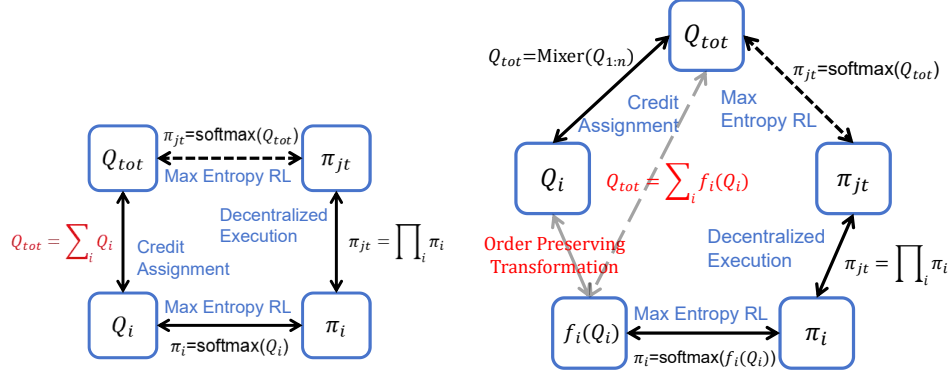


Figure 1: Soft-QMIX combines the QMIX value decomposition mechanism with maximum entropy RL under the CTDE framework. The figure explains the algorithm design rationale. The left figure illustrates a naive approach to applying maximum entropy RL in the CTDE context, where blue text represents the desired objectives, and black text indicates corresponding constraints. It reveals that incorporating maximum entropy RL under the CTDE framework implicitly constrains the global value to be the sum of local values, significantly limiting the expressiveness of the critic network. The right figure depicts the Soft-QMIX improvement, where Soft-QMIX first employs QMIX’s value decomposition mechanism to obtain Q_i . Given the meaningful order of QMIX’s output Q_i , such as possessing properties like IGM, an order-preserving transformation converts Q_i to $f_i(Q_i)$. This transformation is trained by the loss function that minimize the difference between $f_i(Q_i)$ and Q_{tot} .

the landscape of the objective [1], and enhancing robustness [4], has been widely adopted in single-agent RL. However, integrating MARL with maximum entropy RL is not straightforward. As illustrated in Figure 1, using maximum entropy RL within the framework of CTDE will significantly limit the model’s abilities in a manner akin to VDN [28], which enforces that the sum of local q-values must equal the global q-value.

In this paper, we propose a value-based maximum entropy MARL method compatible with the CTDE framework, named Soft-QMIX. We adopt the QMIX [23] mechanism to train a centralized critic network and utilize its credit assignment mechanism to obtain local Q-functions. We also incorporate maximum entropy RL, utilizing stochastic policies and entropy regularization to improve exploration and robustness. To guarantee monotonically increasing expected returns during training and convergence to the optimal policy, an order-preserving transformation on the original local Q-functions is used for the final policy. Through this design, Soft-QMIX can benefit from both maximum entropy RL and QMIX’s credit assignment mechanism, while still ensuring convergence to the optimal strategy.

Our main contributions can be summarized as follows:

- We introduce Soft-QMIX, a value-based maximum entropy MARL algorithm that aligns with the CTDE framework. It employs an order-preserving transformation on local q-values, enabling it to derive meaningful order from credit assignment and leverage the exploratory benefits provided by maximum entropy RL.
- Theoretically, we demonstrate that our approach can monotonically improve the expected q-value and guarantee convergence to the optimal policy.
- Empirically, we confirm the effectiveness of our algorithm through tests on matrix games, MPE [18] and SMAC-v2 [3], where our method attains state-of-the-art results.

2 Related Works

Multi-Agent RL. In the CTDE framework, MARL primarily involves two common algorithmic approaches: policy gradient methods [17, 34, 15, 5, 13, 37] and value function decomposition methods [28, 23, 31]. Policy gradient methods first learn a centralized critic network, and then distill local policies using losses like the KL divergence. On the other hand, Value function decomposition addresses the credit assignment problem by decomposing the global value function into multiple

local value functions. VDN [28] assumes that the global Q-function is the sum of local Q-functions. QMIX [23, 20] permits the mixer function to be any function with non-negative weights. QTRAN [27] optimizes an additional pair of inequality constraints to construct a loss function. QPLEX [31] use the dueling architecture to decompose the Q-function, achieving the same expressive power as QTRAN while being easier to optimize. The expressive power of the critic networks in these algorithms increases sequentially, but experimental results show that QMIX has better performance [9]. Therefore, in this work, QMIX is used as the mechanism for credit assignment.

Maximum Entropy RL. Maximum entropy RL [14] is demonstrated to have advantages such as encouraging exploration [7] and increasing robustness [4] in single-agent RL scenarios. In maximum entropy MARL, most works utilize an actor-critic architecture and typically aim to minimize the KL divergence between the local actor and the centralized critic [8, 6, 22, 36]. However, although these methods employ QMIX to train the critic, they are only capable of minimizing the discrepancy in expectation, thus cannot guarantee the IGM condition, which is central to the QMIX algorithm. Our approach is value-based and ensures that the IGM condition is met while employing maximum entropy MARL. Moreover, our method introduces global information into the local policy during training through a hyper-network, which most previous methods either ignored [35] or only applied in centralized training and centralized execution scenarios [16]. In appendix H, we provide a detailed comparison of our work with related works.

3 Preliminary

3.1 Multi-Agent Reinforcement Learning

Cooperative MARL can be formalized as a Decentralized Partially Observable Markov Decision Process (Dec-POMDP) [19]. Formally, a Dec-POMDP is represented as a tuple $(\mathcal{A}, S, U, T, r, O, G, \gamma)$, where $\mathcal{A} \equiv \{1, \dots, n\}$ is the set of n agents. S, U, O , and γ are state space, action space, observation space, and discount factor, respectively.

During each discrete time step t , each agent $i \in \mathcal{A}$ chooses an action $u^i \in U$, resulting in a collective joint action $\mathbf{u} \in \mathbf{U} \equiv U^n$. The function $r(s, \mathbf{u})$ defines the immediate reward for all agents when the collective action \mathbf{u} is taken in the state s . $\mathcal{P}(s, \mathbf{u}, s') : S \times \mathbf{U} \times S \rightarrow [0, \infty)$ is the state-transition function, which defines the probability density of the succeeding state s' after taking action \mathbf{u} in state s . In a Dec-POMDP, each agent receives only partial observations $o \in O$ according to the observation function $G(s, i) : S \times \mathcal{A} \rightarrow O$. For simplicity, if a function depends on both o^i and s , we will disregard o^i . Each agent uses a policy $\pi_i(u^i|o^i)$ to produce its action u^i from its local observation o^i . Note that the policy should be conditioned on the history $o_{1:t}^i$. For simplicity, we refer to $o_{1:t}^i$ as o_t^i or o^i in the whole paper. The joint policy is denoted as π_{jt} . $\rho_\pi(s_t, \mathbf{u}_t)$ is used to represent the state-action marginals of the trajectory distribution induced by a policy π .

3.2 Individual-Global Condition

In this section, we define two key concepts in credit assignment.

Definition 3.1. Individual-Global-Max (IGM) For joint q -function Q_{tot} , if there exist individual q -functions $[Q_i]_{i=1}^n$ such that the following holds:

$$\arg\max_{\mathbf{u}_t} Q_{tot}(\mathbf{u}_t, s_t) = \begin{pmatrix} \arg\max_{u_t^1} Q_1(u_t^1|o_t^1) \\ \vdots \\ \arg\max_{u_t^n} Q_n(u_t^n|o_t^n) \end{pmatrix}. \quad (1)$$

Then, we say that $[Q_i]_{i=1}^n$ satisfy **IGM** for Q_{tot} under s_t .

In QMIX, to ensure the validity of IGM, the algorithm constrains the expressive capability of Q_{tot} to the following form: $\frac{\partial Q_{tot}}{\partial Q_i} \geq 0, \forall i \in \mathcal{A}$. Restricting the capacity of Q_{tot} using the above inequality results in Q_{tot} being a monotonic function. The monotonicity constraint serves as a sufficient, but not necessary, condition for IGM. Consequently, the monotonicity constraint is more stringent than those required by IGM.

Definition 3.2. Individual-Global-Independence (IGI) For joint policy π_{jt} , if there exist individual policies $[\pi_i]_{i=1}^n$ such that the following holds:

$$\pi_{jt}(\mathbf{u}_t | s_t) = \prod_{i=1}^n \pi_i(u_t^i | o_t^i). \quad (2)$$

Then, we say that $[\pi_i]_{i=1}^n$ satisfies **IGI** for π_{jt} under s_t .

Definition 3.1 characterizes the properties we expect a deterministic policy to possess. Definition 3.2, on the other hand, describes the independence of decision-making among agents during decentralized execution. **IGI** and the **IGO** [36] condition are very similar; we show in Appendix B that **IGI** is a sufficient condition for **IGO**.

3.3 Naive Maximum Entropy MARL Algorithm

In this section, we informally introduce a naive MARL algorithm. We use it to illustrate the issue that naively applying credit assignment to the maximum entropy RL algorithm will lead to limited credit assignment capability.

Assume a value-based framework, where Q_i denotes the local Q-function and the function for credit assignment is denoted as f^c . Hence, the global Q-function, Q_{tot} , can be expressed as $Q_{tot}(\mathbf{u}, s) = f^c(Q_1(u^1, o^1), \dots, Q_n(u^n, o^n), s)$. Based on maximum entropy RL, the global policy is defined as $\pi_{jt}(\cdot | s) \propto \text{softmax}(Q_{tot}(\cdot, s))$ and the local policy as $\pi_i(\cdot | o^i) \propto \text{softmax}(f_i^t(Q_i(\cdot, o^i), s))$, where f_i^t is an arbitrary function. Due to the IGI condition, we have $f^c(Q_1, \dots, Q_n, s) = \sum_{i=1}^n f_i^t(Q_i, s)$. When f_i^t is an identity mapping, the aforementioned algorithm is equivalent to VDN [28]. When f_i^t represents a linear transformation, the algorithm becomes analogous to the DOP, an actor-critic method [33]. In fact, f_i^t can be any function of u^i and o^i , but cannot be a function of u^j or o^j , where $j \neq i$. This constraint limits the expressiveness of the critic network.

4 Soft-QMIX

In this paragraph, we first briefly introduce the motivation behind the Soft-QMIX algorithm. Then, we detail the process of the Soft-QMIX algorithm and show that the expected returns of the centralized training are monotonically increasing and converge to the optimum. Finally, we propose a practical algorithm.

4.1 Motivation

As shown in Figure 2, we divide the decision-making process into two stages (green and blue blocks). In the first stage, agents rank the Q-values for all actions. We employ the value decomposition mechanism from QMIX to obtain local Q-values but only utilize the order of their outputs, not the specific Q-function values. In the second stage, without changing the order, we assign specific Q-values corresponding to each action. When selecting actions in decentralized execution, only the maximum value is required, necessitating just the first stage for execution. The second stage serves primarily to obtain an accurate estimated q-value. During this phase, we can utilize global information, as it is only used during training.

4.2 Soft Policy Iteration

The objective function of Maximum Entropy RL can be represented in the following form:

$$J(\pi_{jt}) = \mathbb{E}_{(s_t, \mathbf{u}_t) \sim \rho_{\pi_{jt}}} \left[r(s_t, \mathbf{u}_t) + \sum_{t=1}^{\infty} \gamma^t (r(s_t, \mathbf{u}_t) + \alpha H(\pi_{jt}(\cdot | s_t))) \right], \quad (3)$$

where $H(\pi_{jt})$ denotes the entropy of the joint policy π_{jt} , and the temperature parameter α is used to control the degree of randomness in the policy.

In the policy evaluation step, we aim to approximate the objective function described in Equation 3 using $Q_{tot} : S \times \mathbf{U} \rightarrow \mathbb{R}$. The soft state value function $V_{tot} : S \rightarrow \mathbb{R}$ is defined as follows:

$$V_{tot}(s) = \mathbb{E}_{\mathbf{u} \sim \pi_{jt}(\cdot | s)} [Q_{tot}(s, \mathbf{u}) - \alpha \log \pi_{jt}(\mathbf{u} | s)]. \quad (4)$$

Repeatedly applying the Bellman operation to update Q_{tot} results in the soft Q_{tot} function for policy π_{jt} . The Bellman operation is defined as follows:

$$\mathcal{T}^{\pi_{jt}} Q_{tot}(s, \mathbf{u}) = r(s, \mathbf{u}) + \gamma \mathbb{E}_{s' \sim \mathcal{P}} [V_{tot}(s')]. \quad (5)$$

In reference to the QMIX, a monotonicity constraint is imposed on the capacity of the critic network. Specifically, Q_{tot} can be formulated as follows:

$$Q_{tot}(s, \mathbf{u}) = \text{Mixer} (Q_1(o^1, u^1), \dots, Q_n(o^n, u^n), s). \quad (6)$$

The network structure of the Mixer function is the same as QMIX's, and is elaborated in Appendix G.

Due to the monotonicity constraint, there is moderate error in estimating of Q_{tot} . To enhance the precision of value estimation, we introduce the TD(λ) [24] method. The estimation error between the maximum entropy objective function and the Bellman equation objective can be expressed as follows:

$$\begin{aligned} \delta_t^V &= -Q_{tot}(s_t, \mathbf{u}_t) + r_t + \gamma V_{tot}(s_{t+1}), \\ \epsilon_t^{td(\lambda)} &= \mathcal{T}_\lambda^{\pi_{jt}} Q_{tot}(s_t, \mathbf{u}_t) - Q_{tot}(s_t, \mathbf{u}_t) = \sum_{l=0}^{\infty} (\gamma \lambda)^l \delta_{t+l}^V. \end{aligned} \quad (7)$$

The derivation and implementation details of Equation 7 are provided in Appendix D. When combining off-policy methods with TD(λ), adopting $\lambda > 0$ requires importance sampling corrections [10]. Following previous work [9], we opt for a small λ and assume that $\mathcal{T}_\lambda^{\pi_{jt}}$ is equivalent to $\mathcal{T}^{\pi_{jt}}$ in expectation. For simplicity, we will use $\mathcal{T}^{\pi_{jt}}$ instead of $\mathcal{T}_\lambda^{\pi_{jt}}$ in theoretical discussions.

The following lemma demonstrates that by iteratively applying the Bellman equation, convergence can be achieved towards the maximum entropy objective Q_{tot} for π_{jt} .

Lemma 4.1 (Joint Soft Policy Evaluation). *Let $Q_{jt}^0 : S \times \mathcal{U} \rightarrow \mathbb{R}$ be a bounded mapping where $|\mathcal{U}| < \infty$. Define the iterative process $Q_{tot}^{k+1} = \mathcal{T}^{\pi_{jt}}(Q_{tot}^k)$. It follows that the sequence $\{Q_{tot}^k\}_{k=0}^{\infty}$ converges to the joint soft-Q-function for policy π_{jt} as $k \rightarrow \infty$.*

Proof. See Appendix C. \square

In Section 4.1, it was mentioned that decision-making is divided into two stages. During training, the policy is defined as $\pi_i^{train}(\cdot | o^i, s) = \text{softmax}(f_i^{\text{stage2}}(f_i^{\text{stage1}}(\cdot | o^i), s) / \alpha)$, where f_i^{stage1} is a function dependent on local observations, responsible for the first stage of decision-making. f_i^{stage2} , on the other hand, is a non-linear order-preserving transformation, responsible for the second stage of decision-making. Although π_i^{train} depends on the global state, which conflicts with the definition in Dec-POMDP, it remains a valid option because it is utilized solely during training. In the subsequent paragraph, π will denote π_i^{train} . f_i^{stage2} can be further decomposed into two order-preserving transformations, g_i and f_i . The output of g_i is Q_i , and f_i further transforms Q_i into the final policy. The form of order-preserving transformation (OPT) is as follows:

$$\text{OPT}_i(x, s) = W_{(1 \times d_1)}^2 \sigma(W_{(d_1 \times 1)}^1 x_{(1 \times d_2)} + b^1) + b^2, \quad (8)$$

where d_1 is the hidden dimension, d_2 is the dimension of actions, b^1 and b^2 are the bias, σ is an activation function, and W^1 and W^2 are non-negative weights. The implementation of the order-preserving transformation is similar to QMIX's and is elaborated in Appendix G, where its weights and biases are provided by a hypernetwork. This hypernetwork takes the global state s as input,

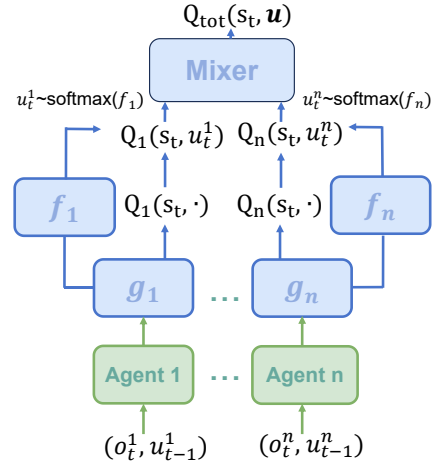


Figure 2: The overall network architecture. Functions g_i and f_i are order-preserving transformations, ensuring the input and output dimensions are identical and have the same argmax values. The output of the f_i function, after undergoing a softmax operation, becomes the policy, from which action u_t^i is sampled. For decentralized execution, only the green network is needed, and the maximum values of their output are selected.

making g_i and f_i functions dependent on the global state. Figure 2 presents the overall framework, where Agents 1 to Agents n correspond to f_i^{stage1} , and g_i and f_i correspond to f_i^{stage2} .

Since g_i is an order-preserving transformation, and $[Q_i]_{i=1}^n$ satisfy the IGM condition for Q_{tot} , it follows that $\arg\max_{\mathbf{u}} Q_{\text{tot}}(\mathbf{u}, s) = \left(\arg\max_{u^1} f_1^{\text{stage1}}(u^1|o^1), \dots, \arg\max_{u^n} f_n^{\text{stage1}}(u^n|o^n) \right)$. Therefore, during execution, only f_i^{stage1} is needed.

During policy improvement, we update the joint policy towards the exponential of the joint Q-function. We constrain $\pi \in \Pi$, where Π is the family of functions that satisfy the **IGI** condition. In the updating process, the updated policy is projected onto Π . Specifically, the update formula is as follows:

$$\pi_{jt}^{\text{new}} = \arg\min_{\pi'_{jt} \in \Pi} D_{KL} \left(\pi'_{jt}(\cdot|s_t) \left\| \frac{\exp(Q_{\text{tot}}^{\pi_{\text{old}}}(s_t, \cdot)/\alpha)}{Z^{\pi_{\text{old}}}(s_t)} \right\| \right), \quad (9)$$

where $Z^{\pi_{\text{old}}}(s_t) = \int_{\mathbf{u}} \exp(Q_{\text{tot}}^{\pi_{\text{old}}}(s_t, \mathbf{u})/\alpha) d\mathbf{u}$.

In value-based methods, Equation 9 is intractable. Therefore, in the policy improvement step, we update the policy in this way:

$$f_i^{\text{new}} = \arg\min_{f'_i} \frac{1}{2} \left(\sum_i f'_i(Q_i(o_t^i, u_t^i, s_t)) - y_t \right)^2, \quad (10)$$

where y_t can be any unbiased estimate of $\mathbb{E}_{s, \mathbf{u} \sim \pi_{jt}} [\mathcal{T}^{\pi_{jt}} Q_{\text{tot}}(s_t, \mathbf{u}_t)]$. Here, we assume² that $\mathcal{T}^{\pi_{jt}} Q_{\text{tot}}(s_t, \mathbf{u}_t)$ is an unbiased estimate of $\mathbb{E}_{s, \mathbf{u} \sim \pi_{jt}} [\mathcal{T}^{\pi_{jt}} \sum_i f_i(Q_i(s_t, \mathbf{u}_t))]$. Under this assumption, we can replace Q_{θ} and y_t in Theorem 4.2 with $\sum_i f_i(Q_i)$ and Q_{tot} respectively, and get that minimizing the L2 norm described in Equation 10 is equivalent to minimizing the KL divergence described in Equation 9 and minimizing the TD loss of value function at the same time. Therefore, in value-based methods, Equation 10 can be used in place of Equation 9.

Theorem 4.2. *If Q-function is parameterized as Q_{θ} , and V_{θ}, π_{θ} are defined as below:*

$$\begin{aligned} V_{\theta}(s) &:= \alpha \log \mathbb{E}_{s, \mathbf{u} \sim \pi_{jt}} [\exp(Q_{\theta}(s, \mathbf{u})/\alpha)], \\ \pi_{jt\theta}(\mathbf{u}|s) &:= \exp(Q_{\theta}(s, \mathbf{u}) - V_{\theta}(s)/\alpha). \end{aligned} \quad (11)$$

and y_t is an unbiased estimator of $\mathbb{E}_{s, \mathbf{u} \sim \pi_{jt}} [\mathcal{T}^{\pi_{jt}} Q_{\theta}(s_t, \mathbf{u}_t)]$. Then, we have

$$\begin{aligned} &\nabla_{\theta} \mathbb{E}_{s, \mathbf{u} \sim \pi_{jt}} [\|Q_{\theta}(s, \mathbf{u}) - y\|^2] \\ &= \alpha \nabla_{\theta} D_{KL}(\pi_{jt}(\cdot|s) \left\| \frac{\exp(y(\cdot, s)/\alpha)}{Z(s)} \right\|) + \nabla_{\theta} \mathbb{E}_{s, \mathbf{u} \sim \pi_{jt}} [\|V_{\theta}(s) - y\|^2] \end{aligned} \quad (12)$$

Proof. See Appendix E.

The subsequent theorem ensures that updating the policy using Equation 9 results in a monotonic increase of the Q-function under the IGI condition.

Lemma 4.3 (Joint Soft Policy Improvement). *Suppose $\pi_{jt}^{\text{old}} \in \Pi$ and consider π_{jt}^{new} to be the solution to Equation 9. Then $Q^{\pi_{jt}^{\text{new}}}(s_t, \mathbf{u}_t) \geq Q^{\pi_{jt}^{\text{old}}}(s_t, \mathbf{u}_t)$ for all $(s_t, \mathbf{u}_t) \in S \times \mathbf{U}$ with $|\mathbf{U}| < \infty$.*

Proof. See Appendix C.

Theorem 4.4 demonstrates that iteratively applying policy evaluation and policy improvement leads to a globally optimal policy under the IGI condition.

Theorem 4.4 (Joint Soft Policy Iteration). *By continually applying soft policy evaluation and soft policy improvement to any $\pi_{jt} \in \Pi$ converges to a policy π^* such that $Q^{\pi^*}(s_t, \mathbf{u}_t) \geq Q^{\pi}(s_t, \mathbf{u}_t)$ for all $\pi_{jt} \in \Pi$ and $(s_t, \mathbf{u}_t) \in S \times \mathbf{U}$, assuming $|\mathbf{U}| < \infty$.*

Proof. See Appendix C.

²This does not necessarily hold in practical implementations, but the difference between these is a term in the loss function of our algorithm. For further discussion, please see the Appendix F.

4.3 The Soft-QMIX Algorithm

Figure 2 illustrates the network architecture of the Soft-QMIX algorithm, which comprises four types of networks. The Mixer network is responsible for handling credit assignment and is parameterized along with its corresponding hypernetwork as Mixer_θ . The $[g_i]_{i=1}^n$ and $[f_i]_{i=1}^n$ are $2n$ order-preserving transformations, with each g_i, f_i and their corresponding hypernetwork parameterized as $g_{i,\theta}$ and $f_{i,\theta}$. Agents 1 to n share parameters, also referred to as f_i^{stage1} in the previous section, and are parameterized as f_θ^{stage1} . The updated rules for these parameters are described as follows.

Soft-QMIX aims to minimize two loss functions. Mixer_θ , $g_{i,\theta}$ and f_θ^{stage1} are updated using the following loss function:

$$L_Q(\theta) = \frac{1}{2} \left(Q_{\text{tot}_\theta}(s_t, \mathbf{u}_t) - \mathcal{T}_\lambda^{\pi_{j^t}} Q_{\text{tot}}(s_t, \mathbf{u}_t) \right)^2, \quad (13)$$

where $Q_{\text{tot}_\theta}(\mathbf{u}, s) = \text{Mixer}_\theta(g_{1,\theta}(f_\theta^{\text{stage1}}(o^1, u^1), s), \dots, g_{n,\theta}(f_\theta^{\text{stage1}}(o^n, u^n), s), s)$, and $\mathcal{T}_\lambda^{\pi_{j^t}} Q_{\text{tot}}(s_t, \mathbf{u}_t)$ is defined in Equation 7. We utilize the technique of target Q networks to stabilize training, where the target Q network is parameterized as $\bar{\theta}$, with $\bar{\theta}$ being the exponentially weighted moving average of θ . Subsequently, the parameter ϕ is updated using the following formula:

$$L_\pi(\phi) = \frac{1}{2} \left(\sum_{i=1}^n f_{i,\phi}(Q_i(o_t^i, u_t^i), s_t) - Q_{\text{tot}}(s_t, \mathbf{u}_t) \right)^2. \quad (14)$$

In this process, the function $f_{i,\phi}$ takes $Q_i(o_t^i, u_t^i)$ as input, but during backpropagation, gradients are truncated at Q_i . This truncation ensures that this loss function updates only $f_{i,\phi}$. After the update, the policy can be expressed in the following form:

$$\pi_i(u^i | o^i, s) = \text{softmax}\left(\frac{f_i(g_i(f_\theta^{\text{stage1}}(o^i), s), s)}{\alpha}\right) \quad (15)$$

It's important to note that during execution, we only need to call f_θ^{stage1} and apply the argmax operation to it. In this paper, α is fixed during training. Finally, the algorithmic procedure of Soft-QMIX is shown in appendix A.

5 Experiments

In this section, we evaluate our algorithm using matrix games from prior works [27], demonstrating its ability to consistently reach the global optimum. Then, we compare Soft-QMIX with QMIX on MPE [18] and empirically demonstrate Soft-QMIX algorithm achieves state-of-the-art performance on the SMAC-v2 [3] benchmark. We compare our algorithm with four baseline algorithms. **MAPPO** [34] adapts the on-policy, single-agent PPO [26] algorithm for multi-agent use, utilizing a centralized value function. **QMIX** [23] is a value-based method employing a monotonic value decomposition to create multiple local deterministic policies from a shared value function. It uses an ϵ -greedy strategy for exploration. **FOP** [36] implements a maximum entropy policy gradient approach with value factorization similar to QPLEX. **HASAC** [16] offers an alternative multi-agent soft actor-critic framework, facilitating sequential decision-making by agents in a centralized training with centralized execution context. We elaborate implementation details and hyperparameters in Appendix J.

5.1 Matrix Games

In this section, we demonstrate the effectiveness of our algorithm in the classic one-step matrix games. Table 1 presents a classic non-monotonic payoff matrix, often used in past papers [27, 31] to discuss the representational capability of critic networks. QMIX, due to its monotonicity constraint, often incurs moderate errors in fitting such payoff matrices. However, in practice, during the training process, we are primarily concerned with the value estimates of those joint actions that are frequently visited. For suboptimal joint actions with lower Q values, their errors do not significantly impact the estimated expected returns. As we use TD- λ to estimate returns in our experiments, such errors can be further reduced. Conversely, we are more concerned with whether the joint actions with the

highest probability of being selected have the globally maximal value function, as we aim for the highest returns when executing with a deterministic policy. For suboptimal joint actions, we also wish to visit them with a certain probability to ensure adequate exploration.

In the matrix game shown in Table 2, QMIX exhibits high estimation error due to its monotonicity constraints, and its deterministic policy lacks effective exploration, which leads it to learn only suboptimal joint actions with a reward of 0. FOP, with its network structure similar to QPLEX, can accurately estimate value functions, yet the corresponding policy learned tends to select suboptimal joint actions more frequently. Soft-QMIX has smaller estimation errors for optimal joint actions and larger errors for suboptimal ones. However, the joint action with the maximum Q value in Soft-QMIX matches the true optimal joint action, and the local policy has the highest probability of selecting the optimal joint action. Soft-QMIX possesses this capability because its decision-making is divided into two steps, and in the first step, it ensures the order of probabilities of each action being selected in the policy.

Table 1: Payoff matrix of the one-step matrix game.

	A	B	C
A	8	-12	-12
B	-12	0	0
C	-12	0	0

Table 2: (a)-(c) respectively demonstrate the results of Soft-QMIX, FOP, and QMIX in the one-step matrix game. The first row and column display the policies adopted by the row and column players after $10k$ steps of training, respectively. The 3×3 matrix in the bottom right corner represents the Q_{tot} ultimately learned by the algorithm. The results indicate that Soft-QMIX is the only method among all that consistently chooses the optimal action with the highest probability.

	1.	0.	0.
1.	8	-12	-14
0.	-8	-28	-30
0.	-10	-30	-32

(a) result of Soft-QMIX

	.21	.39	.40
.21	8	-12	-12
.40	-12	0	0
.39	-12	0	0

(b) result of FOP

	ϵ	$1-2\epsilon$	ϵ
ϵ	-8.5	-8.5	-8.5
$1-2\epsilon$	-8.5	0.2	0.2
ϵ	-8.5	0.2	0.2

(c) result of QMIX

5.2 Multi-Agent Particle Environment

In this section, we test our algorithm on three customized Multi-Agent Particle Environment(MPE) [18] scenarios and show that Soft-QMIX do better exploration compare to QMIX and ablate through different choice of α . Specifically, we use three different *Spread* map, where in each map, agents are tasked to navigate to all the landmarks without collide with each other. Harder map means longer initial distance between agents and landmarks. Details are available in Appendix I. Table 3 shows that Soft-QMIX significantly outperforms QMIX on the *Hard* and *Medium* map which require more exploration, but shows only a slight advantage on the *Simple* map. Additionally, we find that higher α values enhance exploration and performance. These findings support our methodological claim that integrating maximum entropy RL with MARL algorithms boosts exploration capabilities. For each scenario, we conduct four experiments across five seeds, reporting the average evaluation episode rewards after 10M environment steps and their standard deviation in our results table.

Table 3: Experiment result in three MPE scenarios, where Soft-QMIX has higher performance gain from QMIX on *Hard* and *Medium* map, which need more exploration. Higher α also lead to better exploration and higher performance gain.

eval episode rewards	QMIX	Soft-QMIX(ours)		
		$\alpha = 0.1$	$\alpha = 0.3$	$\alpha = 1.0$
Spread(Hard)	-171.7 ± 3.8	-173.7 ± 3.0	-170.8 ± 3.1	$-168.7 \pm 4.6 (+1.8\%)$
Spread(Medium)	-138.4 ± 2.9	-139.0 ± 2.0	-137.4 ± 3.3	$-134.9 \pm 1.8 (+2.5\%)$
Spread(Simple)	-111.9 ± 1.6	-116.2 ± 2.7	-114.4 ± 2.0	$-111.4 \pm 0.9 (+0.4\%)$

5.3 SMAC-v2

We evaluated Soft-QMIX on the SMACv2 [3] benchmark, including six scenarios: *protoss_5_vs_5*, *terran_5_vs_5*, *zerg_5_vs_5*, *protoss_10_vs_10*, *terran_10_vs_10*, and *zerg_10_vs_10*. The results,

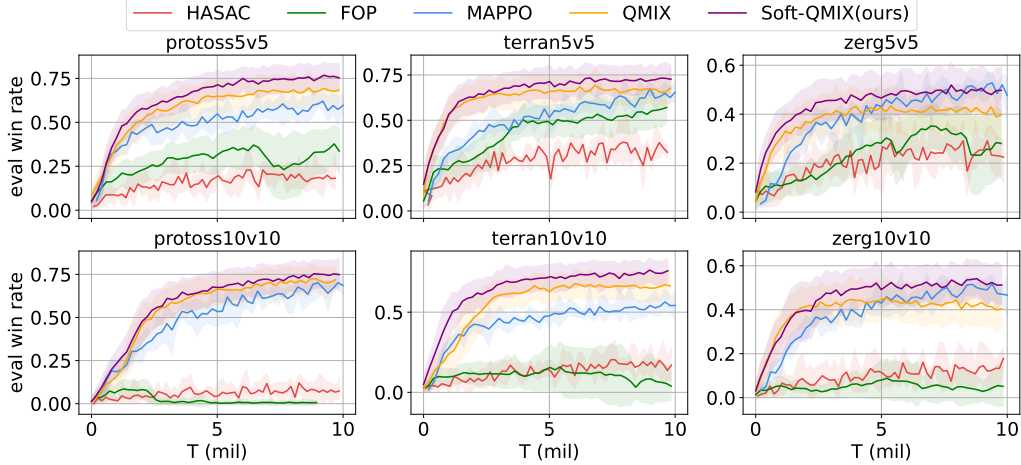


Figure 3: Experiment result in six SMAC-v2 scenarios, where Soft-QMIX achieved faster convergence speed and higher performance compared to baseline algorithms.

as shown in Figure 3, were obtained by training each scenario for 10 million environmental steps, with each curve representing the average of 5 seeds, and HASAC with an average of 3 seeds. Soft-QMIX outperforms the baseline algorithms in all scenarios. MAPPO, being an on-policy algorithm, has lower sampling efficiency, resulting in lower win rates for models trained under 10M environmental steps. Training with MAPPO for 60M environmental steps can achieve win rates comparable to 10M QMIX. QMIX, lacking exploration, tends to converge to local optima, especially in the two Zerg scenarios. HASAC and FOP perform poorly in all the scenarios. Ultimately, Soft-QMIX improves win rates by 5% to 24% in all scenarios compared to baseline algorithms.

5.4 Ablation Study

We evaluate the effectiveness of different components in our algorithm through an ablation study. We begin with QMIX, which utilizes epsilon-greedy exploration. We then introduce **+entropy**, which incorporates softmax sampling (employing $\text{softmax}(Q_i)$ as the policy) along with a maximum entropy objective function to the QMIX framework. Note that this version of the algorithm does not ensure convergence, leading to a performance decline in two out of three scenarios. The subsequent modification, **+function f**, integrates the function f_i (using $\text{softmax}(f_i(Q_i))$ as the policy) building upon the +entropy setup. Empirical results show that function f yields the most substantial performance improvement across all components. Our study culminates with Soft-QMIX, our finalized algorithm. For each modification, we conduct four experiments across three seeds, reporting the average winning rate and its standard deviation in our results table.

Table 4: The ablation studies reveal that each component enhances performance, with function f contributing most significantly to the performance improvement.

eval win rate	QMIX	+entropy	+function f	Soft-QMIX(ours)
protoss 5vs5	0.68 ± 0.04	0.73 ± 0.05	0.74 ± 0.04	0.76 ± 0.04
terran 5vs5	0.68 ± 0.05	0.67 ± 0.04	0.70 ± 0.05	0.72 ± 0.04
zerg 5vs5	0.41 ± 0.05	0.40 ± 0.04	0.48 ± 0.05	0.51 ± 0.04

6 Conclusion

In this paper, we introduced Soft-QMIX, an innovative approach within the CTDE framework, integrating the maximum entropy RL framework with the QMIX-based credit assignment mechanism. Theoretically, we established the monotonic improvement and convergence of Soft-QMIX to a globally optimal solution. Experimentally, our algorithm can solve matrix games and demonstrate state-of-the-art performance on the SMAC-v2 benchmark. Currently, Soft-QMIX is a value-based method, thus one of its limitations is that it can currently only be deployed in tasks with discrete action spaces. In the future, we will try to extend it to tasks with continuous action spaces.

Acknowledgment

This work was supported in part by the U.S. Army Futures Command under Contract No. W519TC-23-C-0030.

References

- [1] Z. Ahmed, N. Le Roux, M. Norouzi, and D. Schuurmans. Understanding the impact of entropy on policy optimization. In *International conference on machine learning*, pages 151–160. PMLR, 2019.
- [2] Y.-H. Chang, T. Ho, and L. Kaelbling. All learning is local: Multi-agent learning in global reward games. *Advances in neural information processing systems*, 16, 2003.
- [3] B. Ellis, J. Cook, S. Moalla, M. Samvelyan, M. Sun, A. Mahajan, J. N. Foerster, and S. Whiteson. Smacv2: An improved benchmark for cooperative multi-agent reinforcement learning. *arXiv preprint arXiv:2212.07489*, 2022.
- [4] B. Eysenbach and S. Levine. Maximum entropy rl (provably) solves some robust rl problems. *arXiv preprint arXiv:2103.06257*, 2021.
- [5] J. Foerster, G. Farquhar, T. Afouras, N. Nardelli, and S. Whiteson. Counterfactual multi-agent policy gradients. In *Proceedings of the AAAI conference on artificial intelligence*, volume 32, 2018.
- [6] F. Guo and Z. Wu. Learning maximum entropy policies with qmix in cooperative marl. In *2022 IEEE 2nd International Conference on Electronic Technology, Communication and Information (ICETCI)*, pages 357–361. IEEE, 2022.
- [7] T. Haarnoja, A. Zhou, K. Hartikainen, G. Tucker, S. Ha, J. Tan, V. Kumar, H. Zhu, A. Gupta, P. Abbeel, et al. Soft actor-critic algorithms and applications. *arXiv preprint arXiv:1812.05905*, 2018.
- [8] Z. He, L. Dong, C. Song, and C. Sun. Multiagent soft actor-critic based hybrid motion planner for mobile robots. *IEEE transactions on neural networks and learning systems*, 2022.
- [9] J. Hu, S. Jiang, S. A. Harding, H. Wu, and S.-w. Liao. Rethinking the implementation tricks and monotonicity constraint in cooperative multi-agent reinforcement learning. *arXiv preprint arXiv:2102.03479*, 2021.
- [10] S. Huang, B. Wang, H. Su, D. Li, J. Hao, J. Zhu, and T. Chen. Off-policy training for truncated td (λ) boosted soft actor-critic. In *Pacific Rim International Conference on Artificial Intelligence*, pages 46–59. Springer, 2021.
- [11] S. Huang, W. Chen, Y. Sun, F. Bie, and W.-W. Tu. Openrl: A unified reinforcement learning framework. *arXiv preprint arXiv:2312.16189*, 2023.
- [12] T. Kim, J. Oh, N. Kim, S. Cho, and S.-Y. Yun. Comparing kullback-leibler divergence and mean squared error loss in knowledge distillation. *arXiv preprint arXiv:2105.08919*, 2021.
- [13] J. G. Kuba, R. Chen, M. Wen, Y. Wen, F. Sun, J. Wang, and Y. Yang. Trust region policy optimisation in multi-agent reinforcement learning. *arXiv preprint arXiv:2109.11251*, 2021.
- [14] S. Levine. Reinforcement learning and control as probabilistic inference: Tutorial and review. *arXiv preprint arXiv:1805.00909*, 2018.
- [15] F. Lin, S. Huang, T. Pearce, W. Chen, and W.-W. Tu. Tizero: Mastering multi-agent football with curriculum learning and self-play. *arXiv preprint arXiv:2302.07515*, 2023.
- [16] J. Liu, Y. Zhong, S. Hu, H. Fu, Q. Fu, X. Chang, and Y. Yang. Maximum entropy heterogeneous-agent mirror learning. *arXiv preprint arXiv:2306.10715*, 2023.

- [17] R. Lowe, Y. I. Wu, A. Tamar, J. Harb, O. Pieter Abbeel, and I. Mordatch. Multi-agent actor-critic for mixed cooperative-competitive environments. *Advances in neural information processing systems*, 30, 2017.
- [18] I. Mordatch and P. Abbeel. Emergence of grounded compositional language in multi-agent populations. In *Proceedings of the AAAI Conference on Artificial Intelligence*, volume 32, 2018.
- [19] F. A. Oliehoek and C. Amato. *A concise introduction to decentralized POMDPs*. Springer, 2016.
- [20] B. Peng, T. Rashid, C. Schroeder de Witt, P.-A. Kamienny, P. Torr, W. Böhmer, and S. Whiteson. Facmac: Factored multi-agent centralised policy gradients. *Advances in Neural Information Processing Systems*, 34:12208–12221, 2021.
- [21] M. S. Pinsker. Information and information stability of random variables and processes. *Holden-Day*, 1964.
- [22] Y. Pu, S. Wang, R. Yang, X. Yao, and B. Li. Decomposed soft actor-critic method for cooperative multi-agent reinforcement learning. *arXiv preprint arXiv:2104.06655*, 2021.
- [23] T. Rashid, M. Samvelyan, C. S. De Witt, G. Farquhar, J. Foerster, and S. Whiteson. Monotonic value function factorisation for deep multi-agent reinforcement learning. *The Journal of Machine Learning Research*, 21(1):7234–7284, 2020.
- [24] J. Schulman, P. Moritz, S. Levine, M. Jordan, and P. Abbeel. High-dimensional continuous control using generalized advantage estimation. *arXiv preprint arXiv:1506.02438*, 2015.
- [25] J. Schulman, X. Chen, and P. Abbeel. Equivalence between policy gradients and soft q-learning. *arXiv preprint arXiv:1704.06440*, 2017.
- [26] J. Schulman, F. Wolski, P. Dhariwal, A. Radford, and O. Klimov. Proximal policy optimization algorithms. *arXiv preprint arXiv:1707.06347*, 2017.
- [27] K. Son, D. Kim, W. J. Kang, D. E. Hostallero, and Y. Yi. Qtran: Learning to factorize with transformation for cooperative multi-agent reinforcement learning. In *International conference on machine learning*, pages 5887–5896. PMLR, 2019.
- [28] P. Sunehag, G. Lever, A. Gruslys, W. M. Czarnecki, V. Zambaldi, M. Jaderberg, M. Lanctot, N. Sonnerat, J. Z. Leibo, K. Tuyls, et al. Value-decomposition networks for cooperative multi-agent learning. *arXiv preprint arXiv:1706.05296*, 2017.
- [29] R. S. Sutton and A. G. Barto. *Reinforcement learning: An introduction*. MIT press, 2018.
- [30] M. Tan. Multi-agent reinforcement learning: Independent vs. cooperative agents. In *Proceedings of the tenth international conference on machine learning*, pages 330–337, 1993.
- [31] J. Wang, Z. Ren, T. Liu, Y. Yu, and C. Zhang. Qplex: Duplex dueling multi-agent q-learning. *arXiv preprint arXiv:2008.01062*, 2020.
- [32] J. Wang, Z. Ren, B. Han, J. Ye, and C. Zhang. Towards understanding cooperative multi-agent q-learning with value factorization. *Advances in Neural Information Processing Systems*, 34: 29142–29155, 2021.
- [33] Y. Wang, B. Han, T. Wang, H. Dong, and C. Zhang. Dop: Off-policy multi-agent decomposed policy gradients. In *International conference on learning representations*, 2020.
- [34] C. Yu, A. Velu, E. Vinitzky, J. Gao, Y. Wang, A. Bayen, and Y. Wu. The surprising effectiveness of ppo in cooperative multi-agent games. *Advances in Neural Information Processing Systems*, 35:24611–24624, 2022.
- [35] M. Zhang, W. Tong, G. Zhu, X. Xu, and E. Q. Wu. Sqix: Qmix algorithm activated by general softmax operator for cooperative multiagent reinforcement learning. *IEEE Transactions on Systems, Man, and Cybernetics: Systems*, 2024.

- [36] T. Zhang, Y. Li, C. Wang, G. Xie, and Z. Lu. Fop: Factorizing optimal joint policy of maximum-entropy multi-agent reinforcement learning. In *International Conference on Machine Learning*, pages 12491–12500. PMLR, 2021.
- [37] Y. Zhong, J. G. Kuba, X. Feng, S. Hu, J. Ji, and Y. Yang. Heterogeneous-agent reinforcement learning, 2023.
- [38] H. Zhou, T. Lan, and V. Aggarwal. Pac: Assisted value factorization with counterfactual predictions in multi-agent reinforcement learning. *Advances in Neural Information Processing Systems*, 35:15757–15769, 2022.

A Soft-QMIX

Algorithm 1 Soft-QMIX

```

1: Input:  $\theta, \phi$ 
2: Initiate:  $\bar{\theta} \leftarrow \theta, D \leftarrow \emptyset$ 
3: for each iteration do
4:   for each environment step do
5:     get  $\pi_i(u_t^i | o_t^i, s_t)$  via Eq. 15
6:      $u_t^i \sim \pi_i(u_t^i | o_t^i, s_t), \forall i \in \{1, \dots, n\}$ 
7:      $s_{t+1} \sim p(s_{t+1} | s_t, \mathbf{u}_t)$ 
8:      $D \leftarrow D \cup \{(s_t, \mathbf{u}_t, r(s_t, \mathbf{u}_t), s_{t+1})\}$ 
9:   end for
10:  for each gradient step do
11:    calculate  $\mathcal{T}_\lambda^{\pi_{jt}} Q_{tot}$  via Eq. 24
12:     $\theta \leftarrow \theta - \lambda_Q \nabla_\theta L_Q(\theta)$ 
13:     $\phi \leftarrow \phi - \lambda_\pi \nabla_\phi L_\pi(\phi)$ 
14:     $\bar{\theta} \leftarrow \tau\theta + (1 - \tau)\bar{\theta}$ 
15:  end for
16: end for

```

B Individual-Global-Independence (IGI)

In this section, we first introduce two concepts, IGI and IGO, where IGI is proposed in our work, and IGO was proposed by A. We then explain that **IGI is a sufficient condition for IGO**.

Definition B.1. Individual-Global-Independence (IGI) For joint policy π_{jt} , if there exist individual policies $[\pi_i]_{i=1}^n$ such that the following holds:

$$\pi_{jt}(\mathbf{u}|s) = \prod_{i=1}^n \pi_i(u^i | o^i). \quad (16)$$

Then, we say that $[\pi_i]_{i=1}^n$ satisfies **IGI** for π_{jt} under s_t .

Definition B.2. Individual-Global-Optimal (IGO) For optimal joint policy π_{jt}^* , if there exist individual optimal policies $[\pi_i^*]_{i=1}^n$ such that the following holds:

$$\pi_{jt}^*(\mathbf{u}|s) = \prod_{i=1}^n \pi_i^*(u^i | o^i). \quad (17)$$

Then, we say that $[\pi_i]_{i=1}^n$ satisfies **IGO** for π_{jt} under s_t .

IGO defines that the optimal joint policy equals the product of optimal local policies. In IGI, it is defined that any joint policy should equal the product of local policies. If finding the optimal policy is viewed as an optimization problem, IGI defines the feasible set of this problem. Hence, any policy not equaling the product of local policies is not a feasible solution and thus cannot be optimal. Therefore, all optimal policies will satisfy the joint policy equals the product of local optimal policies, thereby meeting the IGO condition.

Note that under the assumption of a decentralized execution setting, IGI and IGO are equivalent.

C Joint Policy Iteration

Lemma C.1 (Joint Soft Policy Evaluation). Let $Q_{tot}^0 : S \times \mathbf{U} \rightarrow \mathbb{R}$ be a bounded mapping where $|\mathbf{U}| < \infty$. Define the iterative process $Q_{tot}^{k+1} = \mathcal{T}_\lambda^{\pi_{jt}}(Q_{tot}^k)$. It follows that the sequence $\{Q_{tot}^k\}_{k=0}^\infty$ converges to the joint soft-Q-function for policy π_{jt} as $k \rightarrow \infty$.

Proof. Initiate by defining the entropy-augmented reward function:

$$r_{\pi_{jt}}(s_t, \mathbf{u}_t) := r(s_t, \mathbf{u}_t) + \mathbb{E}_{s_{t+1}} [H[\pi_{jt}(\cdot | s_{t+1})]]. \quad (18)$$

Follow previous work [9], we choose a lower λ and can assume that $\mathcal{T}_\lambda^{\pi_{jt}}$ is an unbiased estimator of $\mathcal{T}^{\pi_{jt}}$. Subsequently, the update mechanism is articulated as:

$$Q_{tot}(s_t, \mathbf{u}_t) \leftarrow r_{\pi_{jt}}(s_t, \mathbf{u}_t) + \gamma \mathbb{E}_{s_{t+1}, \mathbf{u}_{t+1} \sim \pi_{jt}} [Q_{tot}(s_{t+1}, \mathbf{u}_{t+1})]. \quad (19)$$

Conclude by invoking the established convergence theorems pertinent to policy evaluation as explicated by Sutton and Barto. \square

Lemma C.2 (Joint Soft Policy Improvement). *Suppose $\pi_{jt}^{old} \in \Pi$ and consider π_{jt}^{new} to be the solution to Equation 9. Then $Q^{\pi_{jt}^{new}}(s_t, \mathbf{u}_t) \geq Q^{\pi_{jt}^{old}}(s_t, \mathbf{u}_t)$ for all $(s_t, \mathbf{u}_t) \in S \times \mathbf{U}$ with $|\mathbf{U}| < \infty$.*

Proof. Let $\pi_{jt}^{old} \in \Pi$ and let $Q^{\pi_{jt}^{old}}$ and $V^{\pi_{jt}^{old}}$ be the corresponding soft state-action value and soft state value. The update rule of π_{new} can be defined as

$$\begin{aligned} \pi_{new}(\cdot | s_t) &= \arg \min_{\pi' \in \Pi} D_{KL} \left(\pi'(\cdot) \parallel \exp(Q^{\pi_{jt}^{old}}(s_t, \cdot)) - \log Z^{\pi_{jt}^{old}}(s_t) \right) \\ &= \arg \min_{\pi' \in \Pi} J_{\pi_{jt}^{old}}(\pi'(\cdot | s_t)). \end{aligned} \quad (20)$$

Since we can always choose $\pi_{new} = \pi_{old} \in \Pi$, the following inequality always hold true: $J_{\pi_{jt}^{old}}(\pi_{new}(\cdot | s_t)) \leq J_{\pi_{jt}^{old}}(\pi_{jt}^{old}(\cdot | s_t))$. Hence

$$\begin{aligned} &\mathbb{E}_{\mathbf{u}_t \sim \pi_{jt}^{new}} \left[\log(\pi_{jt}^{new}(\mathbf{u}_t | s_t)) - Q^{\pi_{jt}^{old}}(s_t, \mathbf{u}_t) + \log Z^{\pi_{jt}^{old}}(s_t) \right] \\ &\leq \mathbb{E}_{\pi_{jt}^{old}} \left[\log(\pi_{jt}^{old}(\mathbf{u}_t | s_t)) - Q^{\pi_{jt}^{old}}(s_t, \mathbf{u}_t) + \log Z^{\pi_{jt}^{old}}(s_t) \right], \end{aligned} \quad (21)$$

and the inequality reduces to the following form since partition function $Z^{\pi_{jt}^{old}}$ depends only on the state,

$$\mathbb{E}_{\mathbf{u}_t \sim \pi_{jt}^{new}} \left[Q^{\pi_{jt}^{old}}(s_t, \mathbf{u}_t) - \log \pi_{jt}^{new}(\mathbf{u}_t | s_t) \right] \geq V^{\pi_{jt}^{old}}(s_t). \quad (22)$$

Next, consider the soft Bellman equation:

$$\begin{aligned} Q^{\pi_{jt}^{old}}(s_t, \mathbf{u}_t) &= r(s_t, \mathbf{u}_t) + \gamma \mathbb{E}_{s_{t+1} \sim p} \left[V^{\pi_{jt}^{old}}(s_{t+1}) \right] \\ &\leq r(s_t, \mathbf{u}_t) + \gamma \mathbb{E}_{s_{t+1} \sim p} \left[\mathbb{E}_{\mathbf{u}_{t+1} \sim \pi_{jt}^{new}} \left[Q^{\pi_{jt}^{old}}(s_{t+1}, \mathbf{u}_{t+1}) - \log \pi_{jt}^{new}(\mathbf{u}_{t+1} | s_{t+1}) \right] \right] \\ &\vdots \\ &\leq Q^{\pi_{jt}^{new}}(s_t, \mathbf{u}_t), \end{aligned} \quad (23)$$

where we can repeatedly expand $Q^{\pi_{jt}^{old}}$ on the RHS by applying the soft Bellman equation and the bound in Equation 23. Convergence to $Q^{\pi_{jt}^{new}}$ follows from Lemma B.1. \square

Theorem C.3 (Joint Soft Policy Iteration). *By continually applying joint soft policy evaluation and joint soft policy improvement to any $\pi_{jt} \in \Pi$ converges to a policy π_{jt}^* such that $Q^{\pi_{jt}^*}(s_t, \mathbf{u}_t) \geq Q^{\pi_{jt}}(s_t, \mathbf{u}_t)$ for all $\pi_{jt} \in \Pi$ and $(s_t, \mathbf{u}_t) \in S \times \mathbf{U}$, assuming $|\mathbf{U}| < \infty$.*

Proof. Let π_{jt}^i represent the policy after the i -th update. By Lemma B.2, the sequence $Q^{\pi_{jt}^i}$ is monotonically increasing. Given that Q^π is bounded above for $\pi_{jt} \in \Pi$ due to bounded rewards and entropy terms, the sequence converges to some π_{jt}^* . It remains to demonstrate that the policy π_{jt}^* is indeed the optimal policy. At convergence, we infer that $J_{\pi_{jt}^*}(s) \geq J_{\pi_{jt}}(s)$ for all $\pi_{jt} \in \Pi$, if $\pi_{jt} \neq \pi_{jt}^*$. Using the same iterative argument as in the proof of Lemma B.2, we get $Q^{\pi_{jt}^*}(s, \mathbf{u}) \geq Q^\pi(s, \mathbf{u})$ for all $(s, \mathbf{u}) \in S \times \mathbf{U}$, that is, the soft value of any other policy in Π is lower than that of the converged policy. Hence π_{jt}^* is optimal in Π . \square

D TD(λ)

In this paragraph, we will derive the expression of TD(λ) in the context of Maximum Entropy Reinforcement Learning. Specifically, we aim to demonstrate the derivation of the following equation:

$$\mathcal{T}_\lambda^{\pi_{jt}} Q_{tot}(s_t, \mathbf{u}_t) - Q_{tot}(s_t, \mathbf{u}_t) = \sum_{l=0}^{\infty} (\gamma\lambda)^l \delta_{t+l}^V \quad (24)$$

where $\delta_t^V = -Q_{tot}(s_t, \mathbf{u}_t) + r_t + \gamma V_{tot}(s_{t+1})$.

Proof. The one-step TD error can be expressed in the following form:

$$\begin{aligned} \delta_t^V &= -Q_{tot}(s_t, \mathbf{u}_t) + r_t + \gamma V_{tot}(s_{t+1}) \\ \delta_{t+1}^V &= -Q_{tot}(s_{t+1}, \mathbf{u}_{t+1}) + r_{t+1} + \gamma V_{tot}(s_{t+2}) \end{aligned} \quad (25)$$

Next, the k-step TD error can be represented in the following form:

$$\begin{aligned} \epsilon_t^{(1)} &:= -Q_{tot}(s_t, \mathbf{u}_t) + r_t + \gamma V_{tot}(s_{t+1}) = \delta_t^V \\ \epsilon_t^{(2)} &:= -Q_{tot}(s_t, \mathbf{u}_t) + r_t + \gamma r_{t+1} - \log \pi_{jt}(\mathbf{u}_{t+1} | s_{t+1}) + \gamma^2 V_{tot}(s_{t+1}) = \delta_t^V + \gamma \delta_{t+1}^V \\ \epsilon_t^{(k)} &= \sum_{l=0}^{k-1} \gamma^l \delta_{t+l}^V \end{aligned} \quad (26)$$

$$\begin{aligned} \epsilon_t^{td(\lambda)} &:= (1 - \lambda) \left(\epsilon_t^{(1)} + \lambda \epsilon_t^{(2)} + \lambda^2 \epsilon_t^{(3)} + \dots \right) \\ &= (1 - \lambda) \left(\delta_t^V + \lambda (\delta_t^V + \gamma \delta_{t+1}^V) + \lambda^2 (\delta_t^V + \gamma \delta_{t+1}^V + \gamma^2 \delta_{t+2}^V) + \dots \right) \\ &= (1 - \lambda) \left(\delta_t^V (1 + \lambda + \lambda^2 + \dots) + \gamma \delta_{t+1}^V (\lambda + \lambda^2 + \dots) + \gamma^2 \delta_{t+2}^V (\lambda^2 + \lambda^3 + \lambda^4 + \dots) + \dots \right) \\ &= (1 - \lambda) \left(\delta_t^V \left(\frac{1}{1 - \lambda} \right) + \gamma \delta_{t+1}^V \left(\frac{\lambda}{1 - \lambda} \right) + \dots \right) \\ &= \sum_{l=0}^{\infty} (\gamma\lambda)^l \delta_{t+l}^V \end{aligned} \quad (27)$$

□

It is important to note that when computing the TD lambda error in the context of a reverse view and maximum entropy reinforcement learning, it is necessary to subtract the $\log(\pi)$ term from the $t + 1$ step's return as well as subtract $\log(\pi)$ from Q_{t+1} in order to obtain results consistent with Equation 27.

E Soft-Q Learning and Policy Gradient

Theorem E.1. If Q -function is parameterized as Q_θ , and V_θ, π_θ are defined as below:

$$\begin{aligned} V_\theta(s) &:= \alpha \log \mathbb{E}_{\mathbf{u} \sim \pi_{j_t}} [\exp(Q_\theta(s, \mathbf{u})/\alpha)], \\ \pi_{j_t\theta}(\mathbf{u}|s) &:= \exp(Q_\theta(s, \mathbf{u}) - V_\theta(s)) / \alpha. \end{aligned} \quad (28)$$

and y_t is an unbiased estimator of $\mathbb{E}_{s, \mathbf{u} \sim \pi_{j_t}} [\mathcal{T}^{\pi_{j_t}} Q_\theta(s_t, \mathbf{u}_t)]$. Then, we have

$$\begin{aligned} \nabla_\theta \mathbb{E}_{s, \mathbf{u} \sim \pi_{j_t}} [\|Q_\theta(s, \mathbf{u}) - y\|^2] \\ = \alpha \nabla_\theta D_{KL}(\pi_{j_t}(\cdot|s) \parallel \frac{\exp(y(\cdot, s)/\alpha)}{Z(s)}) \\ + \nabla_\theta \mathbb{E}_{s, \mathbf{u} \sim \pi_{j_t}} [\|V_\theta(s) - y\|^2] \end{aligned} \quad (29)$$

Proof. The proof is heavily based on [25]. From assumptions described in Eq. 11 we have:

$$Q_\theta(s, \mathbf{u}) = V_\theta(s) + \alpha \log \pi_{j_t\theta}(\mathbf{u}|s) \quad (30)$$

For simplicity, we further define notation Δ_t as below.

$$\Delta_t = \mathcal{T}^{\pi_{j_t}} Q_\theta(s_t, \mathbf{u}_t) - Q_\theta(s_t, \mathbf{u}_t).$$

From assumption, we have y_t is an unbiased estimator of $\mathbb{E}_{s, \mathbf{u} \sim \pi_{j_t}} [\mathcal{T}^{\pi_{j_t}} Q_\theta(s_t, \mathbf{u}_t)]$. Thus, the relationship between Δ_t and y_t can be written as:

$$\begin{aligned} \mathbb{E}_{s, \mathbf{u} \sim \pi_{j_t}} [y_t] &= \mathbb{E}_{s, \mathbf{u} \sim \pi_{j_t}} [\mathcal{T}^{\pi_{j_t}} Q_\theta(s_t, \mathbf{u}_t)] \\ &= \mathbb{E}_{s, \mathbf{u} \sim \pi_{j_t}} [Q_\theta(s_t, \mathbf{u}_t) + \Delta_t] \\ &= \mathbb{E}_{s, \mathbf{u} \sim \pi_{j_t}} [V_\theta(s_t) + \alpha \mathbb{E}_{\mathbf{u} \sim \pi_{j_t}(\cdot|s)} [\log \pi_{j_t\theta}(\mathbf{u}_t|s_t)] + \Delta_t]. \end{aligned} \quad (31)$$

Here are two equations that will be used in the following proof:

$$\begin{aligned} \mathbb{E}_{s, \mathbf{u} \sim \pi_{j_t\theta}} [(\nabla_\theta V_\theta(s)) (\alpha \log \pi_{j_t\theta}(\mathbf{u}|s))] \\ = \mathbb{E}_{s, \mathbf{u} \sim \pi_{j_t\theta}} [(\nabla_\theta V_\theta(s)) (\alpha \mathbb{E}_{\mathbf{u} \sim \pi_{j_t}(\cdot|s)} [\log \pi_{j_t\theta}(\mathbf{u}|s)])]. \end{aligned} \quad (32)$$

$$\begin{aligned} \mathbb{E}_{a \sim \pi} [\nabla \log \pi(a) f(s)] &= f(s) \sum_a \pi(a) \frac{\nabla \pi(a)}{\pi(a)} \\ &= f(s) \sum_a \nabla \pi(a) = f(s) \nabla \sum_a \pi(a) = 0, \end{aligned} \quad (33)$$

where f can be any function that does not conditioned on a , and $\sum_a \pi(a) = 1$. Let's consider the gradient of the Q -function's MSE loss:

$$\begin{aligned}
& \nabla_{\theta} \mathbb{E}_{s_t, \mathbf{u}_t \sim \pi_{j_t \theta}} \left[\frac{1}{2} (Q_{\theta}(s_t, \mathbf{u}_t) - y_t)^2 \right] \Big|_{\pi = \pi_{\theta}} \\
&= \mathbb{E}_{s_t, \mathbf{u}_t \sim \pi_{j_t \theta}} [\nabla_{\theta} Q_{\theta}(s_t, \mathbf{u}_t) (Q_{\theta}(s_t, \mathbf{u}_t) - y_t)] \Big|_{\pi = \pi_{\theta}} \\
&= \mathbb{E}_{s_t, \mathbf{u}_t \sim \pi_{j_t \theta}} [\nabla_{\theta} Q_{\theta}(s_t, \mathbf{u}_t) (V_{\theta}(s_t) + \alpha \log \pi_{j_t \theta}(\mathbf{u}_t | s_t) - y_t)] \\
&= \mathbb{E}_{s_t, \mathbf{u}_t \sim \pi_{j_t \theta}} [\nabla_{\theta} Q_{\theta}(s_t, \mathbf{u}_t) (V_{\theta}(s_t) + \alpha \log \pi_{j_t \theta}(\mathbf{u}_t | s_t) - V_{\theta}(s_t) - \alpha \mathbb{E}_{\mathbf{u} \sim \pi_{j_t}(\cdot | s)} [\log \pi_{j_t \theta}(\mathbf{u}_t | s_t)] - \Delta_t)] \\
&= \mathbb{E}_{s_t, \mathbf{u}_t \sim \pi_{j_t \theta}} [\nabla_{\theta} Q_{\theta}(s_t, \mathbf{u}_t) (\alpha \log \pi_{j_t \theta}(\mathbf{u}_t | s_t) - \alpha \mathbb{E}_{\mathbf{u} \sim \pi_{j_t}(\cdot | s)} [\log \pi_{j_t \theta}(\mathbf{u}_t | s_t)] - \Delta_t)] \\
&= \mathbb{E}_{s_t, \mathbf{u}_t \sim \pi_{j_t \theta}} [(\nabla_{\theta} V_{\theta}(s_t) + \alpha \nabla_{\theta} \log \pi_{j_t \theta}(\mathbf{u}_t | s_t)) (\alpha \log \pi_{j_t \theta}(\mathbf{u}_t | s_t) - \alpha \mathbb{E}_{\mathbf{u} \sim \pi_{j_t}(\cdot | s)} [\log \pi_{j_t \theta}(\mathbf{u}_t | s_t)] - \Delta_t)] \\
&= \mathbb{E}_{s_t, \mathbf{u}_t \sim \pi_{j_t \theta}} [(\nabla_{\theta} V_{\theta}(s_t)) (\alpha \log \pi_{j_t \theta}(\mathbf{u}_t | s_t)) - (\nabla_{\theta} V_{\theta}(s_t)) (\alpha \mathbb{E}_{\mathbf{u} \sim \pi_{j_t}(\cdot | s)} [\log \pi_{j_t \theta}(\mathbf{u}_t | s_t)]) \\
&\quad - (\nabla_{\theta} V_{\theta}(s_t)) \Delta_t + (\alpha \nabla_{\theta} \log \pi_{j_t \theta}(\mathbf{u}_t | s_t)) (\alpha \log \pi_{j_t \theta}(\mathbf{u}_t | s_t)) \\
&\quad - (\alpha \nabla_{\theta} \log \pi_{j_t \theta}(\mathbf{u}_t | s_t)) (\alpha \mathbb{E}_{\mathbf{u} \sim \pi_{j_t}(\cdot | s)} [\log \pi_{j_t \theta}(\mathbf{u}_t | s_t)]) - (\alpha \nabla_{\theta} \log \pi_{j_t \theta}(\mathbf{u}_t | s_t)) \Delta_t] \\
&= \mathbb{E}_{s_t, \mathbf{u}_t \sim \pi_{j_t \theta}} [- (\nabla_{\theta} V_{\theta}(s_t)) \Delta_t + (\alpha \nabla_{\theta} \log \pi_{j_t \theta}(\mathbf{u}_t | s_t)) (\alpha \log \pi_{j_t \theta}(\mathbf{u}_t | s_t)) - \\
&\quad (\alpha \nabla_{\theta} \log \pi_{j_t \theta}(\mathbf{u}_t | s_t)) (\alpha \mathbb{E}_{\mathbf{u} \sim \pi_{j_t}(\cdot | s)} [\log \pi_{j_t \theta}(\mathbf{u}_t | s_t)]) - (\alpha \nabla_{\theta} \log \pi_{j_t \theta}(\mathbf{u}_t | s_t)) \Delta_t] \\
&= \mathbb{E}_{s_t, \mathbf{u}_t \sim \pi_{j_t \theta}} [- (\nabla_{\theta} V_{\theta}(s_t)) \Delta_t + (\alpha \nabla_{\theta} \log \pi_{j_t \theta}(\mathbf{u}_t | s_t)) (\alpha \log \pi_{j_t \theta}(\mathbf{u}_t | s_t)) - (\alpha \nabla_{\theta} \log \pi_{j_t \theta}(\mathbf{u}_t | s_t)) \Delta_t].
\end{aligned}$$

for simplicity, we ignore the $|\pi = \pi_{\theta}$ after the first two lines of equations. The second equation use Eq. 30. The third equation use Eq. 31. The fourth equation canceled out $V_{\theta}(s_t)$. The fifth equation use Eq. 30 again. The sixth equation expand out terms. The seventh equation use Eq. 32. The last equation use Eq. 33.

Let's consider the gradient of the KL divergence.

$$\begin{aligned}
& \nabla_{\theta} \alpha D_{KL}(\pi_{j_t}(\cdot | s) \| \frac{\exp(y(\cdot, s)/\alpha)}{Z(s)}) \\
&= \nabla_{\theta} \mathbb{E}_{\pi_{j_t}} [\alpha \log \pi_{j_t}(\mathbf{u} | s) - y(\mathbf{u}, s) + \alpha \log Z(s)] \\
&= \nabla_{\theta} \mathbb{E}_{\pi_{j_t}} [\alpha \log \pi_{j_t}(\mathbf{u} | s) - y(\mathbf{u}, s)] \\
&= \nabla_{\theta} [\alpha \sum_{\mathbf{u}} \pi_{j_t}(\mathbf{u} | s) \log \pi_{j_t}(\mathbf{u} | s)] - \nabla_{\theta} [\sum_{\mathbf{u}} \pi_{j_t}(\mathbf{u} | s) y(\mathbf{u}, s)] \\
&= \alpha \sum_{\mathbf{u}} \nabla_{\theta} \pi_{j_t}(\mathbf{u} | s) \log \pi_{j_t}(\mathbf{u} | s) - \sum_{\mathbf{u}} \nabla_{\theta} \pi_{j_t}(\mathbf{u} | s) y(\mathbf{u}, s) \\
&= \mathbb{E}_{\pi_{j_t}} [\alpha (\nabla_{\theta} \log \pi_{j_t}(\mathbf{u} | s)) \log \pi_{j_t}(\mathbf{u} | s) - (\nabla_{\theta} \log \pi_{j_t}(\mathbf{u} | s)) y(\mathbf{u}, s)].
\end{aligned}$$

Note that $V_{\theta}(s) + \alpha \mathbb{E}_{\mathbf{u} \sim \pi_{j_t}(\cdot | s)} [\log \pi_{j_t \theta}(\mathbf{u} | s)]$ is not a function of \mathbf{u} . With Eq. 33, we have:

$$\begin{aligned}
& \nabla_{\theta} \alpha D_{KL}(\pi_{j_t}(\cdot | s) \| \frac{\exp(y(\cdot, s)/\alpha)}{Z(s)}) \\
&= \mathbb{E}_{\pi_{j_t}} [\alpha (\nabla_{\theta} \log \pi_{j_t}(\mathbf{u} | s)) \log \pi_{j_t}(\mathbf{u} | s) - (\nabla_{\theta} \log \pi_{j_t}(\mathbf{u} | s)) \Delta_t]
\end{aligned} \tag{34}$$

Finally, we got:

$$\begin{aligned}
& \nabla_{\theta} \mathbb{E}_{s_t, \mathbf{u}_t \sim \pi_{j_t \theta}} \left[\frac{1}{2} (Q_{\theta}(s_t, \mathbf{u}_t) - y_t)^2 \right] \Big|_{\pi = \pi_{\theta}} \\
&= \nabla_{\theta} \alpha^2 D_{KL}(\pi_{j_t}(\cdot | s_t) \| \frac{\exp(y(s)/\alpha)}{Z(s)}) + \frac{1}{2} \nabla_{\theta} \mathbb{E}_{s_t, \mathbf{u}_t \sim \pi_{j_t \theta}} [(V_{\theta}(s_t) - y_t)^2],
\end{aligned}$$

where $y(s)$ is the distribution of y_t at state s .

□

F Unbiased Assumption

We assume that $\mathcal{T}^{\pi_{jt}} Q_{tot}(s_t, \mathbf{u}_t)$ is an unbiased estimate of $E_{s, \mathbf{u} \sim \pi_{jt}} [\mathcal{T}^{\pi_{jt}} \sum_i f_i(Q_i(s_t, \mathbf{u}_t))]$ in the main paper. Practically, this assumption might fail, leading to non-monotonic increases in the policy improvement step. Here, we initially explain the impact of this error and derive an upper bound for it.

Conclusion: the error's upper bound is proportional to $|Q_{tot} - \sum_i f_i(Q_i)|$ and $\sqrt{D_{KL}(\pi_{jt}^{\text{old}} | \pi_{jt}^{\text{new}})}$. We use Equation 14 as the loss function, ensuring that the first term decreases throughout training. Additionally, by selecting a sufficiently small learning rate, the second term will also remain minimal.

Derivative: We can replace both Q_θ and y_t in Theorem 4.2 with $\sum_i f_i(Q_i)$, and get that minimizing the L2 norm described in Equation 10 is equivalent to minimizing the td loss of value function and minimizing the KL divergence described as follow,

$$\pi_{jt}^{\text{new}} = \arg \min_{\pi_{jt} \in \Pi} D_{KL} \left(\pi_{jt}'(\cdot | s_t) \left\| \frac{\exp(\sum_i f_i(Q_i^{\pi_{jt}^{\text{old}}}(o_t^i, \cdot)/\alpha))}{Z^{\pi_{jt}^{\text{old}}}(s_t)} \right. \right), \quad (35)$$

where $Z^{\pi_{jt}^{\text{old}}}(s_t) = \int_{\mathbf{u}} \exp(\sum_i f_i(Q_i^{\pi_{jt}^{\text{old}}}(o_t^i, u^i))/\alpha) d\mathbf{u}$ and the value function is define as $V'(s) = \sum_i f_i(Q_i(o^i, u^i)) - \alpha \log \pi_{jt}(\mathbf{u} | s)$.

Similar to Equation 22, during policy improvement step, we have:

$$\mathbb{E}_{\mathbf{u}_t \sim \pi_{jt}^{\text{new}}} \left[\sum_i f_i(Q_i^{\pi_{jt}^{\text{old}}}(o_t^i, u_t^i)) - \log \pi_{jt}^{\text{new}}(\mathbf{u}_t | s_t) \right] \leq V'^{\pi_{jt}^{\text{old}}}(s_t). \quad (36)$$

During policy evaluation step, we have:

$$\begin{aligned} Q_{tot}^{\pi_{jt}^{\text{old}}}(s_t, \mathbf{u}_t) &= r(s_t, \mathbf{u}_t) + \gamma \mathbb{E}_{s_{t+1} \sim p} \left[V_{tot}^{\pi_{jt}^{\text{old}}}(s_{t+1}) \right] \\ &= r(s_t, \mathbf{u}_t) + \gamma (\mathbb{E}_{s_{t+1} \sim p} [V'^{\pi_{jt}^{\text{old}}}(s_{t+1})] + \epsilon_1) \\ &\leq r(s_t, \mathbf{u}_t) + \gamma \mathbb{E}_{s_{t+1}} [\mathbb{E}_{\mathbf{u}_{t+1} \sim \pi_{jt}^{\text{new}}} [\sum_i f_i(Q_i^{\pi_{jt}^{\text{old}}}(o_{t+1}^i, u_{t+1}^i)) - \log \pi_{jt}^{\text{new}}(\mathbf{u}_{t+1} | s_{t+1})]]] + \gamma \epsilon_1 \\ &= r(s_t, \mathbf{u}_t) + \gamma \mathbb{E}_{s_{t+1}} [\mathbb{E}_{\mathbf{u}_{t+1} \sim \pi_{jt}^{\text{new}}} [Q_{tot}^{\pi_{jt}^{\text{old}}}(s_{t+1}, \mathbf{u}_{t+1}) - \log \pi_{jt}^{\text{new}}(\mathbf{u}_{t+1} | s_{t+1})]]] + \gamma (\epsilon_1 + \epsilon_2) \\ &\vdots \\ &\leq Q_{tot}^{\pi_{jt}^{\text{new}}}(s_t, \mathbf{u}_t) + \epsilon, \end{aligned} \quad (37)$$

where ϵ is s the cumulative sum of ϵ_1 and ϵ_2 over time. ϵ_1 and ϵ_2 are defined as follows:

$$\begin{aligned} \epsilon_1 &= \mathbb{E}_{s_{t+1} \sim p} \left[V_{tot}^{\pi_{jt}^{\text{old}}}(s_{t+1}) - V'^{\pi_{jt}^{\text{old}}}(s_{t+1}) \right] \\ \epsilon_2 &= \mathbb{E}_{s_{t+1} \sim p} [\mathbb{E}_{\mathbf{u}_{t+1} \sim \pi_{jt}^{\text{new}}} [\sum_i f_i(Q_i^{\pi_{jt}^{\text{old}}}(o_{t+1}^i, u_{t+1}^i)) - Q_{tot}^{\pi_{jt}^{\text{old}}}(s_{t+1}, \mathbf{u}_{t+1})]]] \end{aligned} \quad (38)$$

Then, we have:

$$\begin{aligned}
\epsilon_1 + \epsilon_2 &= \mathbb{E}_{s_{t+1} \sim p} \left[V_{tot}^{\pi_{jt}^{\text{old}}}(s_{t+1}) - V'^{\pi_{jt}^{\text{old}}}(s_{t+1}) \right] \\
&\quad + \mathbb{E}_{s_{t+1} \sim p} \left[\mathbb{E}_{\mathbf{u}_{t+1} \sim \pi_{jt}^{\text{new}}} \left[\sum_i f_i(Q_i^{\pi_{jt}^{\text{old}}}(o_{t+1}^i, u_{t+1}^i)) - Q_{tot}^{\pi_{jt}^{\text{old}}}(s_{t+1}, \mathbf{u}_{t+1}) \right] \right] \\
&= \mathbb{E}_{s_{t+1} \sim p} \left[\mathbb{E}_{\mathbf{u}_{t+1} \sim \pi_{jt}^{\text{old}}} \left[Q_{tot}^{\pi_{jt}^{\text{old}}}(s_{t+1}, \mathbf{u}_{t+1}) - \sum_i f_i(Q_i^{\pi_{jt}^{\text{old}}}(o_{t+1}^i, u_{t+1}^i)) \right] \right] \\
&\quad + \mathbb{E}_{s_{t+1} \sim p} \left[\mathbb{E}_{\mathbf{u}_{t+1} \sim \pi_{jt}^{\text{new}}} \left[\sum_i f_i(Q_i^{\pi_{jt}^{\text{old}}}(o_{t+1}^i, u_{t+1}^i)) - Q_{tot}^{\pi_{jt}^{\text{old}}}(s_{t+1}, \mathbf{u}_{t+1}) \right] \right] \\
&= \mathbb{E}_{s_{t+1} \sim p} \left[\sum_{\mathbf{u}_{t+1}} (\pi_{jt}^{\text{old}}(\mathbf{u}_{t+1}|s_{t+1}) - \pi_{jt}^{\text{new}}(\mathbf{u}_{t+1}|s_{t+1})) (Q_{tot}^{\pi_{jt}^{\text{old}}}(s_{t+1}, \mathbf{u}_{t+1}) - \sum_i f_i(Q_i^{\pi_{jt}^{\text{old}}}(o_{t+1}^i, u_{t+1}^i))) \right] \\
&\leq \mathbb{E}_{s_{t+1} \sim p} \left[C \cdot \sum_{\mathbf{u}_{t+1}} (\pi_{jt}^{\text{old}}(\mathbf{u}_{t+1}|s_{t+1}) - \pi_{jt}^{\text{new}}(\mathbf{u}_{t+1}|s_{t+1})) \right],
\end{aligned} \tag{39}$$

where $C = \arg \max_{\mathbf{u}_{t+1}} |Q_{tot}^{\pi_{jt}^{\text{old}}}(s_{t+1}, \mathbf{u}_{t+1}) - \sum_i f_i(Q_i^{\pi_{jt}^{\text{old}}}(o_{t+1}^i, u_{t+1}^i))|$. Due to the Pinsker's inequality [21], we have:

$$\begin{aligned}
|\epsilon_1 + \epsilon_2| &\leq \mathbb{E}_{s_{t+1} \sim p} \left[C \cdot \sum_{\mathbf{u}_{t+1}} |\pi_{jt}^{\text{old}}(\mathbf{u}_{t+1}|s_{t+1}) - \pi_{jt}^{\text{new}}(\mathbf{u}_{t+1}|s_{t+1})| \right] \\
&\leq \mathbb{E}_{s_{t+1} \sim p} \left[C \cdot \sqrt{2D_{KL}(\pi_{jt}^{\text{old}}(\cdot|s_{t+1})|\pi_{jt}^{\text{new}}(\cdot|s_{t+1}))} \right]
\end{aligned} \tag{40}$$

G Hyper-network Structure

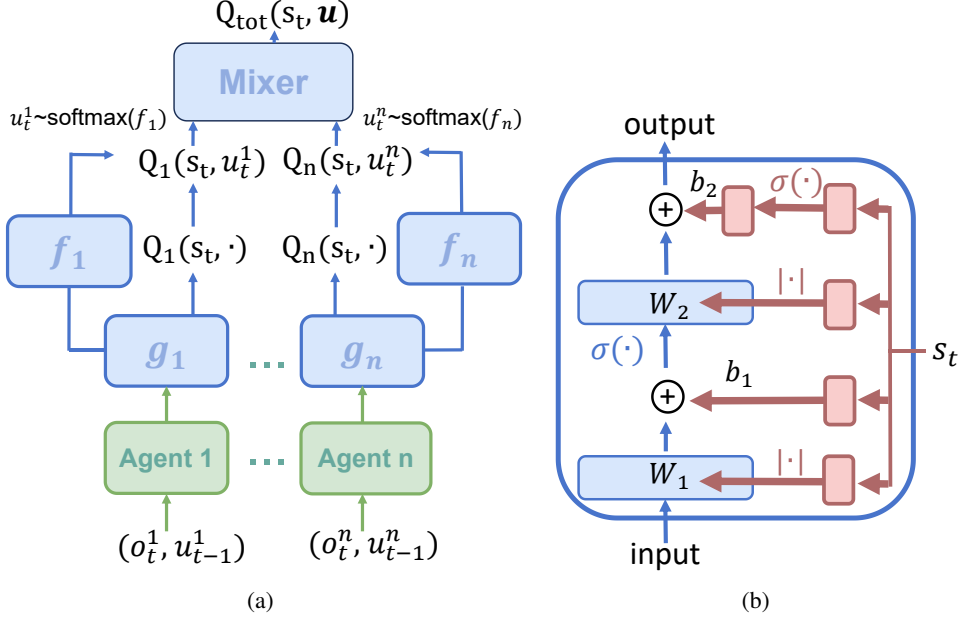


Figure 4: (a) The overall network architecture. Agent 1 to Agent n takes local observations as input and outputs a distribution over local actions u^i . Functions g_i and f_i are order-preserving transformations, ensuring the input and output dimensions are identical and have the same argmax values. Both the input and output of the g_i and f_i networks are k -dimensional, where k is the action dimension. The output of the f_i function, after undergoing a softmax operation, becomes the policy, from which action u_t^i is sampled. The Mixer network takes local Q_i as input and outputs the global Q_{tot} . Green blocks utilize a recurrent neural network as the backbone, with all agents sharing parameters. For decentralized execution, only the green network is needed, and the maximum values of their output are selected. (b) The blue blocks' network structure. The red blocks represent the hyper-network, which takes the global state s_t as input and outputs the network's weights and biases. The weights are constrained to be non-negative. The activation function is denoted by $\sigma(\cdot)$. The mixer network takes an n -dimensional Q function as input and outputs a one-dimensional Q_{tot} .

Figure 4 shows the overall network structure. Specifically, function f_i and function g_i share the same network structure as the mixer network, but while the mixer network's input dimension is (batch_size, agent_num) and its output dimension is (batch_size, 1), both the input and output dimensions of function f_i and function g_i are (batch_size, 1). Additionally, function g_i introduces an additional residual from input to output. The network hyperparameters are as shown in the table below.

layer name	hypernet_embed	embed_dim	num_layer
mixer	64	32	2
function g_i	64	32	2
function f_i	64	-	1

Table 5: Hyper-parameters used for hyper-networks.

H Comparison with Baselines

The following paragraphs present the differences between our method and those based on the AC:

1. Using existing maximum entropy MARL algorithms may result in the loss of action order learned through credit assignment. Achieving the IGM condition, which outlines the order of local value functions, is crucial in credit assignment. Our work presents a value-based algorithm that introduces order-preserving transformations, ensuring that the order of the local actor matches the order of the local value functions. However, the commonly used maximum entropy MARL methods, employing the actor-critic framework, may not guarantee alignment between the actor’s action order and that of the local Q-function due to approximation errors.
2. Actor-critic methods utilize the KL divergence as the loss function, while our approach uses the MSE loss. In the CTDE framework, all methods maintain a more accurate centralized Q-function alongside multiple imprecise local policies. The core idea is to distill knowledge from the centralized Q-function to the local policies. Actor-critic methods typically minimize the KL divergence between the actor and the softmax critic, whereas our method minimizes the MSE loss between their logits. [12] pointed out that, in distillation contexts, MSE is a superior loss function compared to KL divergence.
3. AC methods can use global information when training the critic, resulting in higher model capacity. Our method introduces global information through hyper-networks and the mixer network, which results in lower model capacity.
4. In fact, it’s challenging to theoretically prove that value-based methods are inherently superior to AC methods. However, through experiments, we have demonstrated that our method surpasses both FOP [36] and HASAC [16].

Below are comparisons with individual papers.

mSAC [22] introduces a method similar to MASAC. It employs the AC architecture, thus encountering issues 1 and 2 mentioned above, but does not fully utilize global information to train the critic, hence lacking the advantage noted in point 3.

FOP [36] shares a similar issue with [22], in that the AC framework it utilizes can actually train the critic with global state information. Furthermore, FOP employs a credit assignment mechanism similar to that of QPLEX [31]. [9] experimentally shown that QMIX outperforms QPLEX. Additionally, FOP’s proof concept is that under the IGO conditions, if we locally move local policies towards local optimal policies, the distance between the joint policy and the optimal joint policy also decreases. In contrast, our proof approach first establishes that our method is equivalent to the single-agent SAC algorithm and then completes the proof using existing conclusions.

HASAC [16] is a CTCE version of MASAC, with its core contribution being the introduction of sequential decision-making. Therefore, we do not compare it here.

PAC [38] utilizes global information during centralized training, possessing the advantages noted in point 3. However, it still encounter issues 1 and 2 mentioned above.

I MPE setup

In the MPE [18] *Spread* scenario, three agents and three landmarks are present. Agents work together to cover all landmarks while avoiding collisions. We created three different maps: *Spread(Simple)*, which matches the original benchmark’s *simple_spread*; *Spread(Medium)* and *Spread(Hard)*, which increase the initial distances between agents and landmarks by 1.5X and 2X, respectively.

J Hyper-parameters

For all baseline algorithms, we implemented them using the corresponding open-source frameworks and chose the hyperparameters provided by these frameworks for replication. We used MAPPO implemented by Huang et al., QMIX by Hu et al., FOP by Zhang et al., and HARL by Zhong et al.. Our method, Soft-QMIX, shares the same code base as QMIX. The experiments were conducted on a computer equipped with 92 GB of RAM, a 40-core CPU, and a GeForce RTX 2080 Ti GPU. The following are the hyperparameters used in the experiments.

Hyperparameter	Value
Learning Rate Actor	5e-4
Learning Rate Critic	1e-3
Data Chunk Length	8
Env Num	8
Episode Length	400
PPO Epoch	5
Actor Train Interval Step	1
Use Recurrent Policy	True
Use Adv Normalize	True
Use Value Active Masks	False
Use Linear LR Decay	True

Table 6: MAPPO hyper-parameters used for SMACv2. We utilize the hyperparameters used in SMACv2 [3].

Parameter Name	Value
n_rollout_threads	8
num_env_steps	10000000
warmup_steps	10000
train_interval	50
update_per_train	1
use_valuenorm	False
use_linear_lr_decay	False
use_proper_time_limits	True
hidden_sizes	[256, 256]
activation_func	relu
use_feature_normalization	True
final_activation_func	tanh
initialization_method	orthogonal
gain	0.01
lr	0.0003
critic_lr	0.0005
auto_α	True
α_lr	0.0003
γ	0.99
buffer_size	1000000
batch_size	1000
polyak	0.005
n_step	20
use_huber_loss	False
use_policy_active_masks	True
share_param	False
fixed_order	False

Table 7: HASAC hyper-parameters used for SMACv2. We use the hyperparameters for SMAC as specified in the original paper [16].

Parameter Name	Value
Action Selector	epsilon greedy
ϵ -Start	1.0
ϵ -Finish	0.05
ϵ -Anneal Time	1e5 (5e5 for MPE)
Runner	parallel
Batch Size Run	4
Buffer Size	5000
Batch Size	128
Optimizer	Adam
t_{\max}	1005000
Target Update Interval	200
Mac	n_mac
Agent	n_rnn
Agent Output Type	q
Learner	nq_learner
Mixer	qmix
Mixing Embed Dimension	32
Hypernet Embed Dimension	64
Learning Rate	0.001
λ	0.4

Table 8: QMIX hyper-parameters used for SMACv2 and MPE. We utilize the hyperparameters used in SMACv2 [3].

Parameter Name	Value
$\alpha(5_vs_5)$	0.03
$\alpha(10_vs_10)$	0.005

Table 9: Soft-QMIX hyper-parameters used for SMACv2. Note that besides the hyperparameters mentioned in the table, all other values for Soft-QMIX are the same as those for QMIX.

Parameter Name	Value
Action Selector	Multinomial
ϵ -Start	1.0
ϵ -Finish	0.05
ϵ -Anneal Time	50000
Buffer Size	5000
t_{\max}	1005000
Target Update Interval	200
Agent Output Type	pi_logits
Learner	fop_learner
Head Number	4
Mixing Embed Dimension	32
Learning Rate	0.0005
Burn In Period	100
λ	0.4

Table 10: FOP hyper-parameters used for SMACv2. We use the hyperparameters for SMAC as specified in the original paper [36].

K Impact Statements

This paper presents work whose goal is to advance the field of Machine Learning. There are many potential societal consequences of our work, none which we feel must be specifically highlighted here.